



Published in final edited form as:

Contrast Media Mol Imaging. 2009 July ; 4(4): 183–191. doi:10.1002/cmml.279.

Modulation of Water Exchange in Eu(III) DOTA-tetraamide Complexes: Considerations for *in vivo* imaging of PARACEST agents

Tomoyasu Mani^{†,§}, Gyula Tircso[†], Osamu Togao[§], Piyu Zhao[†], Todd Soesbe[§], Masaya Takahashi[§], and A. Dean Sherry^{†,§}

[†]Department of Chemistry, University of Texas at Dallas, 800 W. Campbell Road, Richardson, TX 75080

[§]Advanced Imaging Research Center, UT Southwestern Medical Center, 5323 Harry Hines Blvd, Dallas, Texas, 75390

Abstract

Modulation of water exchange in lanthanide(III)-DOTA type complexes has drawn considerable attention over the past two decades particularly because of their application as contrast agents for Magnetic Resonance Imaging (MRI). LnDOTA-tetraamide complexes display unusually slow water exchange kinetics and this chemical property offers an opportunity to use these complexes as a new type of contrast agent based upon the chemical exchange saturation transfer (CEST) mechanism. Six new DOTA-tetraamide ligands having side-chain amide arms with varying hydrophobicity and polarity were prepared and the water exchange characteristic of complexes formed with europium (III) complexes were investigated. The results show that introduction of steric bulk into the amide side-chain arms of the europium(III) complexes not only favors formation of the mono-capped twisted square antiprism (TSAP) coordination isomers, the isomer that is generally less favourable for CEST, but also accelerates water exchange in the mono-capped square antiprism (SAP) isomers. However, converting single methyl groups on these bulky arms to carboxyl or carboxyl ethyl esters results in a rather dramatic decrease in water exchange rates, about 50-fold. Thus, steric bulk, polarity, hydrophobicity of the amide side-chains, each contribute to organization of water molecules in the second hydration sphere of the europium(III) ion and this in turn controls water exchange in these complexes.

Keywords

Lanthanide complexes; chemical exchange saturation transfer agents; modulation of water exchange

1. Introduction

Magnetic resonance imaging (MRI) is one of the most powerful and versatile techniques in modern medical diagnostics. MRI contrast originates from differences in tissue proton densities in water and fat and from inherent differences in water relaxation rates. Image contrast can be altered further by administration of a paramagnetic contrast agent, typically a Gd(III) chelate, that shortens the longitudinal relaxation time (T_1) of bulk water protons (1,2). Although first generation contrast agents are now widely used in clinical medicine, the physical properties of such agents are limited in terms of providing physiological, metabolic or functional information

(3). A new type of MRI contrast agent has recently been proposed that alters image contrast by transfer of selectively saturated spins from one chemical pool to another, a process called chemical exchange saturation transfer (CEST) (4–8). To resolve separate CEST exchange peaks, the rate of exchange between the two pools (k_{ex}) must be less than or equal to the frequency difference between the two pools ($\Delta\omega$). Hence, larger $\Delta\omega$ values allow faster exchanging systems to meet the CEST requirement. Large $\Delta\omega$ values have the added benefit of reducing any effects of off-resonance saturation of the bulk water signal. These distinct advantages naturally led to the use of paramagnetic lanthanide ions to induce hyperfine shifts in the proximate exchangeable protons of ligands, an effect commonly referred to as lanthanide induced shifts (LIS). The metal-bound water molecule of Ln(III) DOTA-tetraamide complexes has been shown to exhibit unusually slow water exchange rate and large hyperfine shifts, such that these complexes meet the general slow-to-intermediate exchange guideline, $\Delta\omega \geq k_{ex}$. These exogenous paramagnetic CEST (PARACEST) agents show potential for measuring pH (9), temperature (10), enzyme activity (11,12), metabolites (13,14), metals (15), and tissue glucose (16–18). CEST contrast is achieved by applying a presaturation pulse at the resonance frequency of a slow-intermediate exchanging proton site (-NH, -OH, or metal bound water molecule) of the agent and the resulting saturated or partially saturated spin is transferred to bulk water via chemical exchange. The net effect of CEST is to reduce the bulk water signal intensity detected in an imaging experiment, thereby providing negative contrast in an image similar to that produced by T_2 agents. Since the effectiveness of a CEST agent for providing image contrast is critically dependent upon the water exchange rate (19), modulation of the water exchange rate can be used to create PARACEST agents that respond to physiological or biological events. It has been established that the water exchange process of Ln(III)-bound water molecule on the nine-coordinated complexes (the multidentate ligand occupies eight sites and one coordinated water molecule) occurs through a dissociative pathway (20). The parameters that affect water exchange have been intensively studied over the past decade and found to depend upon the coordination geometry (21–23), steric crowding (24), size of the central ion (25), and the electron density on ligating atoms (26,27). The europium(III) DOTA-tetraamide complexes have shown to have the slowest water exchange rates among other lanthanide(III) DOTA-tetraamide complexes (25). Aime and the coworkers reported that introduction of bulky, hydrophobic substituents on the amide side-chains results in slowing of water exchange (24). This report led to the general hypothesis that the properties of side-chains and the organization of the second hydration sphere around the central Ln(III) ion play major roles in governing water exchange in such complexes.

The central hypothesis of this study was that introduction of bulky alkyl groups into the side-chains of europium(III) DOTA-tetraamide complexes should in general result in slower water exchange and that a simple modification of those same pendant arms to introduce some polarity, i.e., conversion of methyl group to carboxyl and carboxyl ethyl ester group, will further alter water organization in the second hydration sphere around the Eu(III) ion and affect water exchange as well. Subsequently, a series of complexes were prepared that included amide side-chain substituents of varying size (bulkiness) and polarity (*i*-Pr, *t*-Bu, 3-Pentyl, 4-Heptyl, Me₂Gly, Me₂GlyEt) (Figure 1) and the CEST properties and water exchange rates of the resulting europium(III) complexes were investigated both in aqueous solution and in plasma.

2. Results

2.1. High-Resolution ¹H NMR Studies

Lanthanide complexes of DOTA-tetraamide ligands can adopt two coordination geometries in solution that differ in their water exchange kinetics (22,23). The mono-capped square antiprismatic geometry (SAP) typically displays slower water exchange whereas the mono-capped twisted square antiprismatic geometry (TSAP) displays faster water exchange (21–

23,28–30). It has been reported that water exchange in TSAP complexes can be as much as ~50 times faster compared to the corresponding SAP complexes and, for this reason alone, TSAP complexes are less useful as CEST agents (29). Thus, the SAP/TSAP isomer ratio is an important parameter to consider in the development of any new complexes as potential PARACEST agents. The signature of these two coordination isomers is easily seen in high-resolution ^1H NMR spectra of the complexes since a single axial proton on each ethylene unit of the macrocycle (the H4 proton) experiences a large hyperfine shift in Ln(III) DOTA-based complexes and the chemical shift of this H4 proton is quite different in the SAP and TSAP complexes. A comparison of the H4 resonance areas provides a direct readout of the isomer ratio present in solution. For the EuDOTA-tetraamide complexes, the H4 protons are typically found between 24 – 36 ppm in the SAP isomer and between 5 – 12 ppm in the TSAP isomer (31). A distinct H4 proton characteristic of the TSAP coordination isomer was seen in the NMR spectra of all complexes examined in this study, except for Eu(5). The measured SAP/TSAP isomer ratios are summarized in Table 1. The data show that the population of the SAP isomer ranges from a high of near 100 % for the dimethylglycinate analog, Eu(5), to a low of 23 % for the 4-heptyl analog, (Eu(4)). This pattern was somewhat unexpected because the majority of other reported EuDOTA-tetraamide derivatives with bulky amide substituents adopt the SAP conformation nearly exclusively (32). The observation that the TSAP population increases dramatically from Eu(1) ~ Eu(2) < Eu(3) < Eu(4) indicates that introduction of bulky groups on the carbon beta to the amide nitrogen has a substantial impact on the population of the TSAP coordination isomer in solution (Mani, et al., in preparation). Although the TSAP isomer was not detected by NMR in solutions of Eu(5), this isomer must be present in this sample at least to a small extent because the exchange processes that interconvert these isomers, either ring flips or arm rotations, occur even when the concentration of any one isomer is too low to be detected by NMR. It is also interesting to note that a resonance characteristic of a Eu(III)-bound water molecule was not observed in any of the complexes (40 mM) listed in Table 1 when dissolved in pure water at ambient temperatures. This in part indicates that water exchange is faster in all of the complexes reported here in comparison to that observed in EuDOTA-(GlyEt) $_4^{3+}$ where a Eu(III)-bound water signal is detected by high resolution ^1H NMR in pure water solvent at ambient temperatures (7,33).

2.2. CEST studies in water

The most common method for characterizing the CEST properties of such complexes is to apply a long, frequency-selective presaturation pulse over a range of presaturation frequencies followed by an observe pulse to monitor the residual bulk water signal remaining at each frequency. The subsequent plot of residual bulk water signal intensity, M_s/M_0 , as a function of saturation frequency is referred to as a Z-spectrum (34) or, more recently, a CEST spectrum. Such spectra are useful in comparing the CEST properties of such complexes (at equivalent concentrations) and in measuring the water and/or proton exchange rates that contribute to the CEST spectrum. The CEST spectra of this series of complexes differed substantially as the amide substituent was varied from simple alkyl groups to carboxyl groups to esters. The CEST spectra of Eu(2), Eu(5) and Eu(6) are compared in Figure 2. Three conclusions can be reached by simple visual inspection of these three spectra. First, water exchange is fastest in Eu(2) and considerably slower in the two structural analogs, Eu(5) and Eu(6). This shows that the four bulky *t*-butyl groups in Eu(2) do not hinder water access to the inner coordination sphere of the Eu(III) ion but in fact may open and expose the inner-sphere position more to bulk solvent. Conversion of one methyl group on each R group (in Figure 1) to carboxylates (to yield Eu(5)) or carboxyl esters (to yield Eu(6)) slows water exchange substantially. The fitting results are summarized in Table 1. It is important to note that although Eu(1–4) do not strictly satisfy the slow-to-intermediate exchange condition ($\tau_M > \Delta\omega$), one can still derive water exchange rates from their CEST spectra because the broad shoulder on the low field side of their central bulk solvent CEST peaks reflects water exchange in these complexes (37). Interestingly, a plot

of the CEST magnitude for each sample against the water residence lifetime (Figure 3) displays the same general shape as that predicted by exchange theory (8,37).

2.3. Comparison of the CEST properties of the complexes in water versus plasma

In anticipation of using these agents *in vivo*, a series of imaging experiments were first performed on samples of Eu(2), Eu(5) and Eu(6) dissolved in plasma to evaluate whether the presence of proteins alters their CEST properties. CEST images were collected near 20°C (the temperature in the magnet room) as a function of agent concentration and again at a single agent concentration but at various near physiological temperatures. Those results are summarized in Table 2 and Table 3. Although some differences were observed between the images of the Eu(2) samples in plasma versus water at ~20°C, the differences were relatively small for Eu(6) and insignificant for Eu(5). Although Eu(6) has a comparable CEST effect and somewhat slower water exchange than Eu(5), it is known that positively charged molecules such as these are generally toxic *in vivo* (35), presumably because they bind to cell membrane surfaces (negatively charged) and disrupt ion pumps and transport systems. The CEST spectra of 10 mM Eu(5) in water and plasma were not significantly different at 27°C but did differ somewhat at higher temperatures, 35–39°C (Table 3). The 18–25% smaller CEST effect for Eu(5) dissolved in plasma suggests that plasma proteins may alter water exchange in this system at these higher temperatures. The reason for this is not clear at this point, but one could hypothesize that the amide side-chains of the complex may be more accessible to solvent at higher temperatures and this may allow greater interactions between the complex and macromolecules thereby altering water exchange. Acceleration of water exchange by binding to human serum albumin (HSA) has been reported previously (36). The water residence lifetime measured from the CEST spectra of Eu(5) in water at 37°C was 28 μs, considerably shorter than the lifetime measured for this complex at 25°C (104 μs, see Table 1). It is important to note that the *in vitro* results reported here do not necessarily translate to the *in vivo* situation because CEST is also affected by the bulk water relaxation and other tissue factors that may differ from organ to organ; however, these *in vitro* results do serve as a useful guideline.

3. Discussion

The Eu(III) complexes of simple DOTA-monoalkylamides, Eu(1), Eu(2), Eu(3), and Eu(4), show relatively small CEST effects at 40 mM and all four complexes also display the shortest water residence lifetimes (τ_M). An increase in steric bulk of the amide substituent from isopropyl to t-butyl to 3-pentyl to 4-heptyl resulted in shorter water residence lifetimes. According to previously published observations for a series of EuDOTA-tetraamide systems containing bulky benzyl or glycinate ester groups (24), increasing the steric bulk around the Eu(III) coordination sphere was predicted to increase the bound water lifetime. The present results show that this rule cannot be generalized for just any bulky substituent - clearly there are other factors involved. If the model proposed by Aime et al. (24) indicating that a more solvent exposed Eu(III) coordination sphere (accessible surface area around the Eu(III) ion) results in a shorter lifetime, then we must conclude that the bulky groups, i-Pr, tert-Bu, 2-pentyl, and 3-heptyl in Eu(1–4), respectively, experience steric interactions among the side-chains that result in exposure of the Eu(III)-bound water molecule to more bulk solvent thereby lowering the activation energy for water exchange. This conclusion is opposite that predicted by the model of Aime, et al. (24) who concluded that “introduction of a more hydrophobic ligand surface should raise the free energy of the transition state leading to longer water exchange lifetimes”.

In addition to bulk steric effects, a second important factor is polarity of the amide substituent. As suggested in the earlier study, introduction of polar groups should help stabilize second sphere water molecules through hydrogen bonding interactions and that “any substituents on

the ligand which can aid the ingress of the exchanging water (such as those with polar head-groups) should lower the free energy of activation for water exchange". Nevertheless, Eu(III) complexes of DOTA-glycyl-n-butyl ester and DOTA-glycyl-benzyl ester were reported to have the longest bound water lifetimes. To investigate more subtle changes in polarity *versus* steric bulk, we prepared an analog of Eu(2) wherein one methyl group on each side-arm was replaced by a single carboxylate group, yielding Eu(5). This subtle structural change resulted in a 10-fold increase in bound water lifetime, increasing it from 10 μ s in Eu(2) to 104 μ s in Eu(5), both measured at 25°C. Given that the steric requirements of these two molecules should be similar, this indicates that addition of the polar carboxyl group likely stabilizes the second hydration sphere around the Eu(III) ion which, in turn, stabilizes the inner-sphere water molecule resulting in slower water exchange. As one adds hydrophobicity to this polar carboxyl group in the form of an ethyl ester, the water residence lifetime is further lengthened by a factor of two (compare the lifetimes of Eu(5) (104 μ s) and Eu(6) (210 μ s)). This trend highlights the importance of both polarity (Eu(5)) and hydrophobicity (Eu(6)) in slowing water exchange. We suggest that the polar carboxyl groups stabilize the second hydration sphere structure thereby establishing a hydrogen bond network that stabilizes the inner-sphere water molecule while the four hydrophobic ethyl groups likely hinder the access of further incoming water and decrease the number of water molecules available for an exchange with the single inner-sphere Eu(III)-bound water molecule. This model is not only consistent with the data presented here but also consistent with data in (24) where the longest bound water lifetime was found for the polar, yet hydrophobic EuDOTA-glycyl-esters.

As illustrated in Figure 3, the experimentally determined CEST effects for this series correlates with the water residence lifetimes as predicted by exchange theory (8). This experimentally demonstrates that PARACEST agents such as these have an optimal bound water lifetime for CEST at the magnetic field, applied B_1 (23.5 μ T) and temperature (25°C) used to collect these data. Although this relationship indicates that Eu(5) and Eu(6) have near optimal water exchange rates for optimal CEST using these experimental conditions, the observation that the water exchange rate in Eu(5) increases substantially (~4-fold) between 25°C and 37°C means that CEST (M_z/M_0) will be substantially reduced for this compound when it is used *in vivo* (37–39°C in mice). This observation emphasizes the importance of measuring water exchange at 37°C when optimizing the chemistry of the DOTA-tetraamide ligands for *in vivo* use as PARACEST agents.

4. Experimental

4.1. NMR spectroscopy

NMR samples for CEST studies were prepared by dissolving the appropriate amount of the agents in H₂O or human blood plasma (650 μ l). The pH values of the solutions in pure water for CEST experiments were adjusted to near pH 7.4 (to be near physiological conditions) by adding small amount of NaOH or gaseous HCl.

4.2. Fitting CEST spectra to the Bloch equations modified for exchange

The water exchange rates were estimated by fitting the experimental CEST spectra to a three pool (bound water and amide protons exchanging with bulk water) model based on the numerical solutions obtained from modified Bloch equations written in MATLAB (The Mathworks Inc., Natick, MA). This program is available from the authors upon request (37). The applied B_1 field (in Hz) was calibrated prior to collection of the CEST spectra by measuring the 360° pulse width for bulk water protons as a function of transmitter power level. The T_1 of solvent water was measured using a standard inversion recovery sequence without a presaturation pulse while T_2 was estimated from the bulk water linewidth. The following parameters were included in the fitting procedure: applied field (B_1) in Hz, the presaturation

time, concentrations of exchanging bound water protons and amide protons, T_1 (bulk water), T_2 (bulk water), and chemical shifts of the Eu^{3+} -bound water exchange peak and the complex –NH protons. Since CEST was detected only from the SAP isomer as evidenced by a bound water exchange peak near 50 ppm, the concentration of the complex was given as that fraction of the total concentration that exists in solution as the SAP isomer as measured by high resolution NMR (see Table 1). It was assumed that the TSAP isomer when present in solution does not affect the fitting procedure (modeling indicates this is a good assumption – data not shown). The residence lifetime of the $\text{Eu}(\text{III})$ -bound water molecule was determined by averaging the fitting results measured at different B_1 values (9.4, 14.1, 18.8, 23.5 μT) except for $\text{Eu}(\text{IV})$ where the CEST effect was small even using an applied field of 23.5 μT . Initial estimates of τ_M (bound water lifetime) were given along with an upper and lower boundary values, typically 10–500 μs .

4.3. CEST Imaging of Phantoms

The europium complexes were dissolved either in water or in human plasma containing NaEDTA (Innovative Research, Novi, Michigan, USA) at various concentrations of agent. CEST imaging was performed at 9.4 T using a standard spin echo imaging sequence preceded by a 5 s presaturation hard pulse ($B_1 = 14.1 \mu\text{T}$). The frequency of the presaturation pulse was set either on the $\text{Eu}(\text{III})$ -bound water resonance frequency of each molecule (“on-resonance”) or at an equal frequency upfield of the water resonance (“off-resonance”). The difference in water intensities between these two spectra was defined as $\text{CEST} (\%) = (SI_{\text{off}} - SI_{\text{on}}) / SI_{\text{off}} \times 100$.

4.4. General procedures

All reagents and solvents were purchased from commercial source and used as received, unless otherwise stated. ^1H NMR and ^{13}C NMR were recorded on either a JEOL Eclipse 270 spectrometer operating at 270.17 MHz and 67.5 MHz, or a Bruker Avance III 400 spectrometer operating at 400.13 MHz and 100.03 MHz, respectively. High resolution ^1H NMR and Z-spectra were recorded on a Varian Inova 500 spectrometer operating at 500 MHz. Infrared spectra were recorded using a PerkinElmer 1600 Fourier Transform IR spectrometer. Melting points were recorded on a Fisher/Johns melting point apparatus and are uncorrected.

4.5. Synthesis

4.5.1. 2-Bromo-N-isopropyl-acetamide, (arm-1)—*iso*-Propylamine (5.0 g, 84.6 mmol) and potassium carbonate (35 g, 0.254 mol) were dissolved in dichloromethane (200 ml). The mixture was cooled to 0 °C, and a solution of 2-bromoacetyl bromide (8.08 ml, 93.0 mmol) was added drop-wise with stirring over half an hour. The reaction mixture was stirred at room temperature for 2 h and then quenched with water (200 mL). The reaction mixture was transferred to a separatory funnel, and the two phases were separated; the organic layer was washed with a 5% citric acid solution (200 mL) and then with water (200 mL). The organic extract was dried (Na_2SO_4) and the solvents were removed *in vacuo*. The solid residue was dried under vacuum to afford the title compound as a colorless solid (9.59 g, 63 %); mp: 62–64 °C. ^1H NMR (400 MHz, CDCl_3): δ 1.12 (6H, d, $^3J_{\text{H-H}} = 6.4$ Hz, $\text{CH}(\text{CH}_3)_2$), 3.78 (2H, s, BrCH_2CO), 3.96 (1H, hept, $^3J_{\text{H-H}} = 6.4$ Hz, $\text{CH}(\text{CH}_3)_2$), 6.20 (1H, s br, NH). ^{13}C NMR (67.5 MHz, CDCl_3): δ 22.4 ($\text{C}(\text{CH}_3)_3$), 29.4 ($\text{C}(\text{CH}_3)_3$), 42.3 (BrCH_2CO), 164.4 ($\text{C}=\text{O}$) IR $\nu_{\text{max}}/\text{cm}^{-1}$ (KBr Disc): 3286 (NH), 3080, 3023, 2974, 2391, 2875, 1646 (C=O), 1559, 1458, 1420, 1386, 1367, 1214, 1169, 1131, 989, 934, 891, 847, 709, 656, 563.

4.5.2. Tetrakis-(N-iso-propyl)-1,4,7,10-tetraazacyclododecane-1,4,7,10-tetracetamide - DOTA-(i-propyl-amide) $_4$, (1)—1,4,7,10-tetraazacyclododecane (1.00 g, 5.8 mmol) and potassium carbonate (9.63 g, 69.7 mol) were dissolved in anhydrous acetonitrile

(200 mL) with stirring under N₂ followed by the addition of arm-1 (4.23 g, 23.5 mmol) at ambient temperature over half an hour. The reaction mixture was stirred at 65 °C for 48 h. After cooling the reaction mixture was filtered. The solvents were removed *in vacuo*. The residue was dissolved in hot methanol (200 mL) and the mixture was filtered and the solvents removed *in vacuo*. The residue was washed with icy water and the solid was dried under vacuum and then recrystallized from acetonitrile to afford the title compound as a colorless solid (2.45 g, 74 %); mp: 234–236 °C. ¹H NMR (400 MHz, CD₃OD): δ 1.04 (36H, d, ³J_{H-H} = 6.4 Hz, CH(CH₃)₂), 2.93 (16H, s br, ring NCH₂), 3.21 (8H, s, NCH₂CO), 3.84 (4H, hept, CH(CH₃)₂). ¹³C NMR (100 MHz, CD₃OD): δ 22.7 (C(CH₃)₃), 42.3 (CH(CH₃)₂), 52.1 (ring NCH₂), 59.2 (NCH₂CO), 172.0 (C=O). IR ν_{max}/cm⁻¹ (KBr Disc): 3448 (NH), 3228 (NH), 3060, 2973, 2931, 2832, 1650 (C=O), 1538, 1466, 1452, 1321, 1302, 1267, 1244, 1227, 1172, 1131, 1103, 1021, 963, 933, 809, 701, 602. *m/z* (ESI-MS⁺): 570 ([M+H]⁺, 100%), 592 ([M+Na]⁺, 50%), 664 ([M+K]⁺, 40%). Anal. Calcd for C₂₈H₅₆N₈O₄·9HCl: C, 37.5; H, 7.3; N, 12.5. Found: C, 37.3; H, 6.9; N, 12.3%.

4.5.3. 2-Bromo-N-tert-butyl-acetamide, (arm-2)—The title compound was synthesized in an analogous manner to that described for arm-1 using *tert*-Butylamine (10.0 g, 0.137 mol). The compound was obtained as a colorless solid (23.14 g, 87 %); mp: 76–78 °C. ¹H NMR (270 MHz, CDCl₃): δ 1.32 (9H, s, NC(CH₃)₃), 3.73 (2H, s, BrCH₂CO), 6.31 (1H, s br, NH). ¹³C NMR (67.5 MHz, CDCl₃): δ 28.5 (C(CH₃)₃), 29.9 (C(CH₃)₃), 51.9 (BrCH₂CO), 164.6 (C=O). IR ν_{max}/cm⁻¹ (KBr Disc): 3309 (NH), 3074, 3011, 2977, 2931, 2869, 1679 (C=O), 1651 (C=O), 1551, 1476, 1452, 1426, 1389, 1359, 1320, 1208, 1141, 934, 779, 676, 653, 575.

4.5.4. Tetrakis-(N-tert-butyl)-1,4,7,10-tetraazacyclododecane-1,4,7,10-tetracetamide - DOTA-(t-Bu-amide)₄, (2)—The title compound was synthesized in an analogous manner to that described for 1 using arm-2 (9.98 g, 50.4 mmol). The compound was obtained as a colorless solid (8.08 g, 91 %); mp: 222–224 °C. ¹H NMR (270 MHz, CD₃OD): δ 1.32 (36H, s, C(CH₃)₃), 2.90 (16H, s br, ring NCH₂), 3.30 (8H, s, NCH₂CO), 7.42 (4H, s, NH). ¹³C NMR (67.5 MHz, CD₃OD): δ 27.7 (C(CH₃)₃), 50.3 (ring NCH₂), 50.6 (C(CH₃)₃), 58.1 (NCH₂CO), 170.8 (C=O). IR ν_{max}/cm⁻¹ (KBr Disc): 3513 (NH), 3284 (NH), 3053, 2968, 2933, 2823, 1673 (C=O), 1537, 1456, 1393, 1367, 1308, 1226, 1101, 1024, 952, 591. *m/z* (ESI-MS⁺): 626 ([M+H]⁺, 6%), 648 ([M+Na]⁺, 4%), 664 ([M+K]⁺, 100%). Anal. Calcd for C₃₂H₆₄N₈O₄·4HCl: C, 49.9; H, 8.9; N, 14.5. Found: C, 49.4; H, 8.6; N, 13.8%.

4.5.5. 2-Bromo-N-(1-ethyl-propyl)-acetamide, (arm-3)—The title compound was synthesized in an analogous manner to that described for arm-1 using 3-Pentylamine (6.69 ml, 57.4 mmol). The compound as a colorless solid (9.76 g, 81 %); mp: 53–54 °C. ¹H NMR (400 MHz, CDCl₃): δ 0.825 (6H, t, ³J_{H-H} = 7.6 Hz, CH₂CH₃), 1.30 (2H, m, ³J_{H-H} = 7.6 Hz, CHCH_aH_bCH₃), 1.47 (2H, m, ³J_{H-H} = 5.2 Hz, CHCH_aH_bCH₃), 3.66 (1H, m, ³J_{H-H} = 5.6 Hz, CH(CH₂CH₃)₂), 3.83 (2H, s, BrCH₂CO), 6.10 (1H, s br, NH). ¹³C NMR (100 MHz, CDCl₃): δ 10.1 (CH₂CH₃), 27.2 (CH₂CH₃), 29.6 (CH(CH₂CH₃)₂), 52.9 (BrCH₂CO), 164.9 (C=O). IR ν_{max}/cm⁻¹ (KBr Disc): 3282 (NH), 3087, 3020, 2968, 2934, 2876, 1647 (C=O), 1560, 1458, 1438, 1379, 1322, 1265, 1213, 1161, 1147, 952, 928, 788, 721, 649, 565.

4.5.6. Tetrakis-(N-(1-ethyl-propyl))-1,4,7,10-tetraazacyclododecane-1,4,7,10-tetracetamide - DOTA-(3-pentyl-amide)₄, (3)—1,4,7,10-tetraazacyclododecane (1.00 g, 5.80 mmol) and potassium carbonate (9.63 g, 69.6 mmol) were dissolved in dry acetonitrile anhydrous (200 mL) with stirring under N₂ atmosphere followed by the addition of arm-3 (4.89 g, 23.5 mmol) at ambient temperature over half an hour. The reaction mixture was stirred at 65 °C for 48 h. The reaction mixture was then filtered and the solid residues were dissolved in hot ethanol. The mixture was filtered and the solvents were removed *in vacuo* and the solid residue was dried under vacuum to afford the title compound as a colorless solid (1.54 g, 39

); mp: 203–204 °C. ¹H NMR (270 MHz, CDCl₃): δ 0.84 (24H, t, ³J_{H-H} = 7.2 Hz, CH₂CH₃), 1.37 (16H, m, ³J_{H-H} = 6.9 Hz, CH₂CH₃), 2.76 (16H, s br, ring NCH₂), 3.07 (8H, s br, NCH₂CO), 3.71 (4H, m, ³J_{H-H} = 6.9 Hz, CH(CH₂CH₃)₂), 6.70 (4H, s br, CONH). ¹³C NMR (67.5 MHz, CD₃Cl): δ 10.5 (CH₂CH₃), 27.4 (CH₂CH₃), 51.8 (ring NCH₂), 55.3 (NHC(CH₃)₂), 52.8 (NHC(CH₂CH₃)₂), 59.6 (NCH₂CONH), 170 (C=O). IR ν_{max}/cm⁻¹ (KBr Disc): 3295 (NH), 3075, 2961, 2934, 2874, 2859, 2838, 1661 (C=O), 1638 (C=O), 1550, 1525, 1457, 1376, 1326, 1301, 1285, 1142, 1127, 1091, 998, 981, 721, 586. m/z (ESI-MS⁺): 682 ([M+H]⁺, 100%), 704 ([M+Na]⁺, 5%). Anal. Calcd for C₃₆H₇₂N₈O₄: C, 63.5; H, 10.7; N, 16.5. Found: C, 63.2; H, 10.1; N 16.1.

4.5.7. 2-Bromo-N-(1-propyl-butyl)-acetamide, (arm-4)—The title compound was synthesized in an analogous manner to that described for arm-1 using 4-Heptylamine (6.53 ml, 43.4 mmol). The compound was obtained as a colorless solid (9.51 g, 93 %); mp: 69–70 °C. ¹H NMR (400 MHz, CDCl₃): δ 0.90 (6H, t, ³J_{H-H} = 6.4 Hz, CH₂CH₂CH₃), 1.28 (4H, m, ³J_{H-H} = 3.6 Hz, CH₂CH₂CH₃), 1.39 (4H, m, ³J_{H-H} = 6.4 Hz, CH₂CH₂CH₃), 3.89 (2H, s, BrCH₂CO), 3.91 (1H, m, ³J_{H-H} = 3.6 Hz, CH(CH₂CH₂CH₃)₂), 6.15 (1H, d, ³J_{H-H} = 5.6 Hz, NH). ¹³C NMR (100 MHz, CDCl₃): δ 14.0 (CH₂CH₂CH₃), 19.0 (CH₂CH₂CH₃), 29.6 (BrCH₂CO), 37.2 (CH₂CH₂CH₃), 49.8 (CH(CH₂CH₂CH₃)₂), 164.8 (C=O). IR ν_{max}/cm⁻¹ (KBr Disc): 3281 (NH), 3086, 3022, 2958, 2873, 1642 (C=O), 1558, 1463, 1432, 1381, 1323, 1245, 1212, 1146, 971, 900, 745, 714, 665, 588.

4.5.8. Tetrakis-(N-(1-ethyl-propyl))-1,4,7,10-tetraazacyclododecane-1,4,7,10-tetracetamide - DOTA-(4-heptyl-amide)₄, (4)—The title compound was synthesized in an analogous manner to that described for 3 using arm-4 (4.44 g, 18.8 mmol). The compound was obtained as a colorless crystalline solid (3.24 g, 86 %); mp: 175–177 °C. ¹H NMR (270 MHz, CD₃Cl): δ 0.85 (24H, t, ³J_{H-H} = 7.2 Hz, CH₂CH₂CH₃), 1.30 (16H, m, ³J_{H-H} = 3.2 Hz, CH₂CH₂CH₃), 1.39 (16H, m, ³J_{H-H} = 3.2 Hz, CH₂CH₂CH₃), 2.73 (16H, s br, ring NCH₂), 3.03 (8H, s, BrCH₂CO), 3.91 (1H, br, CH(CH₂CH₂CH₃)₂), 6.50 (1H, d, ³J_{H-H} = 9.4 Hz, NH). ¹³C NMR (100 MHz, CDCl₃): δ 14.0 (CH₂CH₂CH₃), 19.3 (CH₂CH₂CH₃), 37.5 (CH₂CH₂CH₃), 48.5 (CH(CH₂CH₂CH₃)₂), 52.8 (ring NCH₂), 59.7 (BrCH₂CO), 167.0 (C=O). IR ν_{max}/cm⁻¹ (KBr Disc): 3305 (NH), 3058, 2956, 2933, 2871, 2815, 1647 (C=O), 1542, 1465, 1378, 1298, 1144, 1117, 1086, 1002, 982, 965, 740, 596. m/z (ESI-MS⁺): 794 ([M+H]⁺, 100%), 815 ([M+Na]⁺, 3%). Anal. Calcd for C₄₄H₈₈N₈O₄.HCl: C, 63.7; H, 10.8; N, 13.5. Found: C, 63.9; H, 10.6; N 13.2.

4.5.9. 2-(2-Bromo-acetyl-amino)-2-methyl-propionic acid tert-butyl ester, (arm-5)—The title compound was synthesized in an analogous manner to that described for arm-1 using 2-Amino-2-methyl-propionic acid tert-butyl ester hydrochloride (5.00 g, 25.6 mmol). The compound was obtained as a colorless solid (6.86 g, 95 %); mp: 55–56 °C. ¹H NMR (270 MHz, CDCl₃): δ 1.46 (9H, s, C(CH₃)₃), 1.56 (6H, s, NHC(CH₃)₂CO), 3.80 (2H, BrCH₂CO), 7.25 (1H, s, NH). ¹³C NMR (67.5 MHz, CDCl₃): δ 24.0 (NHC(CH₃)₂CO), 27.8 (C(CH₃)₃), 29.2 (BrCH₂CO), 57.5 (C(CH₃)₃), 82.3 (NHC(CH₃)₂CO), 164.5 (CH₂CONH), 173.4 (COOC(CH₃)₃). IR ν_{max}/cm⁻¹ (KBr Disc): 3303 (NH), 3059, 3024, 3003, 2985, 2936, 1728 (C=O), 1650, 1541, 1456, 1385, 1325, 1281, 1252, 1219, 1143, 847, 677, 667, 566.

4.5.10. 1,4,7,10-tetraazacyclododecane-1,4,7,10-tetrakis(2-acetoamino-2methyl-propionic acid) - DOTA-(Me₂Gly)₄, (5)—1,4,7,10-tetraazacyclododecane (0.60 g, 3.48 mmol) and potassium carbonate (3.85 g, 27.8 mmol) were dissolved in acetonitrile anhydrous (200 mL) with stirring under N₂ atmosphere followed by the addition of arm-5 (3.95 g, 14.1 mmol) at ambient temperature over half an hour. The reaction mixture was stirred at 65 °C for 48 h. The reaction mixture was then filtered and the solvents were removed *in vacuo*. The solid residue was dissolved in chloroform (100 mL) and

water (100 mL). The mixture was transferred to a separatory funnel, and the two phases were separated; the organic phase was dried (Na_2SO_4), the solvents were removed *in vacuo*. The solid residue was dried under vacuum and *tert*-butyl ester ligand was obtained as colorless solid (2.71 g, 96 %) and used in the next step without further purification. *tert*-Butyl ester ligand (2.70 g, 2.78 mmol) was dissolved in dioxane (25 mL) followed by the addition of saturated HCl in dioxane (65 mL). The reaction mixture was stirred at 55 °C for 48 h. The solvents were removed *in vacuo* and the solid residue dissolved in water (20 mL). The solvents were removed by lyophilization to afford the title compound as a pale blue solid (2.37 g, 93 %); mp: 195–197 °C. ^1H NMR (270 MHz, D_2O): δ 1.45 (24H, s, $\text{C}(\text{CH}_3)_2$), 3.17 (8H, s br, ring NCH_2), 3.30 (8H, s br, ring NCH_2), 3.70 (8H, s br, NCH_2CO). ^{13}C NMR (67.5 MHz, D_2O): δ 24.3 ($\text{NHC}(\text{CH}_3)_2$), 50.2 (ring NCH_2), 55.3 ($\text{NHC}(\text{CH}_3)_2$), 56.4 ($\text{NHC}(\text{CH}_3)_2$), 66.7 (NCH_2CONH), 178 ($\text{C}=\text{O}$). IR $\nu_{\text{max}}/\text{cm}^{-1}$ (KBr Disc): 3360 (OH), 3242 (NH), 3058, 2989, 1731 ($\text{C}=\text{O}$), 1681 ($\text{C}=\text{O}$), 1548, 1472, 1457, 1391, 1365, 1255, 1160, 1086, 608. m/z (ESI-MS⁺): 746 ($[\text{M}+\text{H}]^+$, 100%), 768 ($[\text{M}+\text{Na}]^+$, 28%). Anal. Calcd for $\text{C}_{32}\text{H}_{52}\text{N}_8\text{O}_{12}\cdot 3\text{HCl}\cdot \text{H}_2\text{O}$: C, 44.1; H, 7.1; N, 12.9. Found: C, 43.9; H, 7.5; N 12.9.

4.5.11. 2-(2-Bromo-acetyl-amino)-2-methyl-propionic acid ethyl ester, (arm-6)—

The title compound was synthesized using in an analogous manner to that described for arm-1 using 2-Amino-2-methyl-propionic acid ethyl ester hydrochloride (5.00 g, 25.6 mmol). The compound was obtained as a colorless solid (5.81 g, 77 %); mp: 84–87 °C. ^1H NMR (400 MHz, CDCl_3): δ 1.29 (3H, t, $^3J_{\text{H-H}} = 7$ Hz, OCH_2CH_3), 1.60 (6H, s, $\text{NHC}(\text{CH}_3)_2$), 3.83 (2H, s, BrCH_2CO), 4.23 (2H, q, $^3J_{\text{H-H}} = 7$ Hz, OCH_2CH_3), 7.13 (1H, s, br, NH). ^{13}C NMR (100 MHz, CDCl_3): δ 14.1 (OCH_2CH_3), 24.2 ($\text{NHC}(\text{CH}_3)_2$), 29.1 (BrCH_2CO), 57.2 ($\text{NHC}(\text{CH}_3)_2$), 61.8 (OCH_2CH_3), 164.6 (CONH), 174.2 (COOCH_2). IR $\nu_{\text{max}}/\text{cm}^{-1}$ (KBr Disc): 3259 (NH), 3067, 3004, 2987, 2942, 2873, 1733 ($\text{C}=\text{O}$), 1646 ($\text{C}=\text{O}$), 1549, 1466, 1365, 1331, 1278, 1165, 1111, 1023, 953, 885, 873, 946, 763, 666, 614, 557, 516, 429.

4.5.12. 1,4,7,10-tetraazacyclododecane-1,4,7,10-tetrakis(2-acetoamino-2methyl-propionic acid ethyl ester) - DOTA-(Me₂GlyEt)₄, (6)—

The title compound was synthesized in an analogous manner to that described for 1 using arm-6 (2.96 g, 11.8 mmol). The compound was obtained as a colorless crystalline solid (1.17 g, 47 %); mp: 148–150 °C. ^1H NMR (400 MHz, CDCl_3): δ 1.20 (12H, t, $^3J_{\text{H-H}} = 7$ Hz, OCH_2CH_3), 1.46 (24H, s, $\text{NHC}(\text{CH}_3)_2$), 2.69 (16H, s br, ring NCH_2), 3.10 (8H, s, NCH_2CO), 4.11 (8H, q, $^3J_{\text{H-H}} = 7$ Hz, OCH_2CH_3), 7.75 (4H, s br, NH). ^{13}C NMR (100 MHz, CDCl_3): δ 12.3 (OCH_2CH_3), 23.1 ($\text{NHC}(\text{CH}_3)_2$), 50.3 (ring NCH_2), 54.3 (BrCH_2CO), 57.6 ($\text{NHC}(\text{CH}_3)_2$), 59.6 (OCH_2CH_3), 168.6 (CONH), 172.9 (COOCH_2). IR $\nu_{\text{max}}/\text{cm}^{-1}$ (KBr Disc): 3267, (NH), 3050, 2984, 2937, 2806, 1734 ($\text{C}=\text{O}$), 1651 ($\text{C}=\text{O}$), 1539, 1417, 1454, 1383, 1364, 1276, 1235, 1150, 1112, 1027, 601. m/z (ESI-MS⁺): 858 ($[\text{M}+\text{H}]^+$, 100%). Anal. Calcd for $\text{C}_{40}\text{H}_{72}\text{N}_8\text{O}_{12}$: C, 56.1; H, 8.5; N, 13.1. Found: C, 55.7; H, 8.4; N 12.9.

4.5.13. Europium(III) Tetrakis-(N-iso-propyl)-1,4,7,10-tetraazacyclododecane-1,4,7,10-tetracetamide, (Eu(1))—

The ligand DOTA-(iPro-amide)₄ (0.100 g, 0.176 mmol) was dissolved in methanol (5 mL) followed by the addition of a 0.562 M aqueous solution of Europium(III) chloride (0.31 mL, 0.176 mmol). The mixture was stirred at 50 °C for 48 h. The solution was evaporated to dryness by heating at 85 °C. The solid residue was taken up into water (5 mL) and was filtered through a 2 μm membrane filter. Lyophilization of the resulting clear solution afforded the title compound as a colorless solid which was used in NMR studies without further purification; m/z (ESI-MS⁺): 721 ($[\text{M}+\text{H}]^+$, 100%), 756 ($[\text{M}+\text{Na}]^+$, 10%).

4.5.14. Europium(III) Tetrakis-(N-tert-butyl)-1,4,7,10-tetraazacyclododecane-1,4,7,10-tetracetamide, (Eu(2))—

The title compound was

synthesized in an analogous manner to that described for Eu(1) using the ligand **2** (0.101 g, 0.16 mmol); m/z (ESI-MS+): 776 ($[M+H]^+$, 100%), 812 ($[M+Na]^+$, 12%).

4.5.15. Europium(III) Tetrakis-(N-(1-ethyl-propyl))-1,4,7,10-tetraazacyclododecane-1,4,7,10-tetracetamide, (Eu(3))—The title compound was synthesized in an analogous manner to that described for Eu(1) using the ligand **3** (0.200 g, 0.294 mmol); m/z (ESI-MS+): 833 ($[M+H]^+$, 100%), 868 ($[M+Na]^+$, 8%), 904 ($[M+2Na]^+$, 2%).

4.5.16. Europium(III) Tetrakis-(N-(1-ethyl-propyl))-1,4,7,10-tetraazacyclododecane-1,4,7,10-tetracetamide, Eu(4)—The title compound was synthesized in an analogous manner to that described for Eu(1) using the ligand **4** (0.201 g, 0.249 mmol); m/z (ESI-MS+): 944 ($[M-CH_3]^+$, 100%), 980 ($[M-CH_3+Na]^+$, 26%), 1016 ($[M-CH_3+2Na]^+$, 10%).

4.5.17. Europium(III) 1,4,7,10-tetraazacyclododecane-1,4,7,10-tetrakis(2-acetoamino-2methyl-propionic acid), (Eu(5))—The ligand **5** (0.955 g, 1.28 mmol) was dissolved in water (50 mL). a 0.0293 M aqueous solution of Europium(III) chloride (1.4 mL, 38.1 μ mol) was added to the aqueous solution of **2** (2.00 mL, 38.4 μ mol) and the solution was heated at 40 °C. The pH of the solution was then raised to 7 by addition of a dilute potassium hydroxide solution over 2 h. Lyophilization of the resulting clear solution afforded the complex as a colorless solid which was used in NMR studies without further purification; m/z (ESI-MS+): 866 ($[M-HCO]$, 100%), 935 ($[M+Na]$, 74%), 971 ($[M+2Na]^+$, 44%), 1009 ($[M+3Na]^{2+}$, 68%), 1047 ($[M+4Na]^{3+}$, 81%).

4.5.18. Europium(III) 1,4,7,10-tetraazacyclododecane-1,4,7,10-tetrakis(2-acetoamino-2methyl-propionic acid ethyl ester), (Eu(6))—The title compound was synthesized using in an analogous manner to that described for Eu(1) using the ligand **6** (0.100 g, 0.116 mmol); m/z (ESI-MS+): 1008 ($[M-H]^{2+}$, 100%).

Acknowledgments

This research was supported in part by grants from the National Institutes of Health (CA-115531, CA-126608, RR-02584, EB-04582) and the Robert A. Welch Foundation (AT-584).

References

1. Caravan P, Ellison JJ, McMurry TJ, Lauffer RB. Gadolinium(III) Chelates as MRI Contrast Agents: Structure, Dynamics, and Applications. *Chem Rev* 1999;99(9):2293–2352. [PubMed: 11749483]
2. Merbach, AndréE.; Toth, E. *The Chemistry of Contrast Agents in Medical Magnetic Resonance Imaging*. New York: Wiley; 2001.
3. Woods M, Zhang S, Sherry AD. Toward the Design of MR Agents for Imaging β -Cell Function. *Current Medicinal Chemistry - Immunology, Endocrine & Metabolic Agents* 2004;4:349–369.
4. Zhang S, Merritt M, Woessner DE, Lenkinski RE, Sherry AD. PARACEST agents: modulating MRI contrast via water proton exchange. *Acc Chem Res* 2003;36(10):783–790. [PubMed: 14567712]
5. Aime S, Delli Castelli D, Terreno E. Novel pH-reporter MRI contrast agents. *Angew Chem Int Ed Engl* 2002;41(22):4334–4336. [PubMed: 12434381]
6. Ward KM, Aletras AH, Balaban RS. A new class of contrast agents for MRI based on proton chemical exchange dependent saturation transfer (CEST). *J Magn Reson* 2000;143(1):79–87. [PubMed: 10698648]
7. Zhang S, Winter P, Wu K, Sherry AD. A novel europium(III)-based MRI contrast agent. *J Am Chem Soc* 2001;123(7):1517–1518. [PubMed: 11456734]

8. Woods M, Woessner DE, Sherry AD. Paramagnetic lanthanide complexes as PARACEST agents for medical imaging. *Chem Soc Rev* 2006;35(6):500–511. [PubMed: 16729144]
9. Aime S, Barge A, Castelli DD, Fedeli F, Mortillaro A, Nielsen FU, Terreno E. Paramagnetic lanthanide (III) complexes as pH-sensitive chemical exchange saturation transfer (CEST) contrast agents for MRI applications. *Magnetic Resonance in Medicine* 2002;47(4):639–648. [PubMed: 11948724]
10. Zhang S, Malloy CR, Sherry AD. MRI thermometry based on PARACEST agents. *J Am Chem Soc* 2005;127(50):17572–17573. [PubMed: 16351064]
11. Yoo B, Raam MS, Rosenblum RM, Pagel MD. Enzyme-responsive PARACEST MRI contrast agents: a new biomedical imaging approach for studies of the proteasome. *Contrast Media & Molecular Imaging* 2007;2(4):189–198. [PubMed: 17712869]
12. Chauvin T, Durand P, Bernier M, Meudal H, Doan B-T, Noury F, Badet B, Beloeil J-C, Toth E. Detection of Enzymatic Activity by PARACEST MRI: A General Approach to Target a Large Variety of Enzymes13. *Angewandte Chemie International Edition* 2008;47(23):4370–4372.
13. Aime S, Delli Castelli D, Fedeli F, Terreno E. A Paramagnetic MRI-CEST Agent Responsive to Lactate Concentration. *Journal of the American Chemical Society* 2002;124(32):9364–9365. [PubMed: 12167018]
14. Liu G, Li Y, Pagel MD. Design and characterization of a new irreversible responsive PARACEST MRI contrast agent that detects nitric oxide. *Magnetic Resonance in Medicine* 2007;58(6):1249–1256. [PubMed: 18046705]
15. Trokowski R, Ren J, Kalman FK, Sherry AD. Selective Sensing of Zinc Ions with a PARACEST Contrast Agent13. *Angewandte Chemie International Edition* 2005;44(42):6920–6923.
16. Zhang S, Trokowski R, Sherry AD. A paramagnetic CEST agent for imaging glucose by MRI. *J Am Chem Soc* 2003;125(50):15288–15289. [PubMed: 14664562]
17. Trokowski R, Zhang S, Sherry AD. Cyclen-based phenylboronate ligands and their Eu³⁺ complexes for sensing glucose by MRI. *Bioconj Chem* 2004;15(6):1431–1440. [PubMed: 15546212]
18. Ren J, Trokowski R, Zhang S, Malloy CR, Sherry AD. Imaging the tissue distribution of glucose in livers using a PARACEST sensor. *Magn Reson Med* 2008;60(5):1047–1055. [PubMed: 18958853]
19. Zhang, Shanrong; Jiang, Xiuyan; Sherry, AD. Modulation of the Lifetime of Water Bound to Lanthanide Metal Ions in Complexes with Ligands Derived from 1,4,7,10-Tetraazacyclododecane Tetraacetate (DOTA). *Helvetica Chimica Acta* 2005;88(5):923–935.
20. Micskei K, Helm L, Brucher E, Merbach AE. Oxygen-17 NMR study of water exchange on gadolinium polyaminopolyacetates [Gd(DTPA)(H₂O)]²⁻ and [Gd(DOTA)(H₂O)]⁻ related to NMR imaging. *Inorganic Chemistry* 1993;32(18):3844–3850.
21. Aime S, Barge A, Botta M, De Sousa AS, Parker D. Direct NMR Spectroscopic Observation of a Lanthanide-Coordinated Water Molecule whose Exchange Rate Is Dependent on the Conformation of the Complexes. *Angewandte Chemie International Edition* 1998;37(19):2673–2675.
22. Aime S, Barge A, Bruce JI, Botta M, Howard JAK, Moloney JM, Parker D, de Sousa AS, Woods M. NMR, Relaxometric, and Structural Studies of the Hydration and Exchange Dynamics of Cationic Lanthanide Complexes of Macrocyclic Tetraamide Ligands. *Journal of the American Chemical Society* 1999;121(24):5762–5771.
23. Woods M, Kovacs Z, Zhang S, Sherry AD. Towards the Rational Design of Magnetic Resonance Imaging Contrast Agents: Isolation of the Two Coordination Isomers of Lanthanide DOTA-Type Complexes13. *Angewandte Chemie International Edition* 2003;42(47):5889–5892.
24. Aime S, Barge A, Batsanov AS, Botta M, Castelli DD, Fedeli F, Mortillaro A, Parker D, Puschmann H. Controlling the variation of axial water exchange rates in macrocyclic lanthanide(III) complexes. *Chem Commun (Camb)* 2002;10:1120–1121. [PubMed: 12122694]
25. Zhang S, Wu K, Sherry AD. Unusually sharp dependence of water exchange rate versus lanthanide ionic radii for a series of tetraamide complexes. *J Am Chem Soc* 2002;124(16):4226–4227. [PubMed: 11960448]
26. Terreno E, Boniforte P, Botta M, Fedeli F, Milone L, Mortillaro A, Aime S. The Water-Exchange Rate in Neutral Heptadentate DO3A-Like Gd^{III} Complexes: Effect of the Basicity at the Macrocyclic Nitrogen Site. *European Journal of Inorganic Chemistry* 2003;2003(19):3530–3533.

27. Ratnakar SJ, Woods M, Lubag AJ, Kovacs Z, Sherry AD. Modulation of water exchange in europium (III) DOTA-tetraamide complexes via electronic substituent effects. *J Am Chem Soc* 2008;130(1): 6–7. [PubMed: 18067296]
28. Woods M, Aime S, Botta M, Howard JAK, Moloney JM, Navet M, Parker D, Port M, Rousseaux O. Correlation of Water Exchange Rate with Isomeric Composition in Diastereoisomeric Gadolinium Complexes of Tetra(carboxyethyl)dota and Related Macrocyclic Ligands. *Journal of the American Chemical Society* 2000;122(40):9781–9792.
29. Dunand FA, Aime S, Merbach AE. First 17O NMR Observation of Coordinated Water on Both Isomers of [Eu(DOTAM)(H₂O)]³⁺: A Direct Access to Water Exchange and its Role in the Isomerization I. *Journal of the American Chemical Society* 2000;122(7):1506–1512.
30. Port M, Rousseaux O, Raynal I, Woods M, Parker D, Moreau J, Rimbault J, Pierrard JC, Aplincourt M. Synthesis and physicochemical characterization of 1,4,7,10-tetra (2-glutaryl)-1,4,7,10 tetraazacyclododecane lanthanide complexes. *Acad Radiol* 2002;9:S300–S303. [PubMed: 12188254]
31. Adair C, Woods M, Zhao P, Pasha A, Winter PM, Lanza GM, Athey P, Sherry AD, Kiefer GE. Spectral properties of a bifunctional PARACEST europium chelate: an intermediate for targeted imaging applications. *Contrast Media Mol Imaging* 2007;2(1):55–58. [PubMed: 17326038]
32. Woods M, Zhang S, Ebron VH, Sherry AD. pH-Sensitive Modulation of the Second Hydration Sphere in Lanthanide(III) Tetraamide-DOTA Complexes: A Novel Approach to Smart MR Contrast Media. *Chemistry - A European Journal* 2003;9(19):4634–4640.
33. Dixon WT, Ren J, Lubag AJM, Ratnakar J, Vinogradov E, Hancu I, Lenkinski RE, Sherry AD. A concentration-independent method to measure exchange rates in PARACEST agents. *Magn Reson Med*. 2009 in press.
34. Grad J, Bryant R. Nuclear magnetic cross-relaxation spectroscopy. *J Magn Reson* 1990;90:1–8.
35. Lv H, Zhang S, Wang B, Cui S, Yan J. Toxicity of cationic lipids and cationic polymers in gene delivery. *Journal of Controlled Release* 2006;114(1):100–109. [PubMed: 16831482]
36. Ali MM, Woods M, Suh EH, Kovacs Z, Tircso G, Zhao P, Kodibagkar VD, Sherry AD. Albumin-binding PARACEST agents. *J Biol Inorg Chem* 2007;12(6):855–865. [PubMed: 17534672]
37. Woessner DE, Zhang S, Merritt M, Sherry AD. Numerical Solution of the Bloch Equations Provides Insights into the Optimum Design of PARACEST Agents for MRI. *Magn Reson Med* 2005;53:790–799. [PubMed: 15799055]

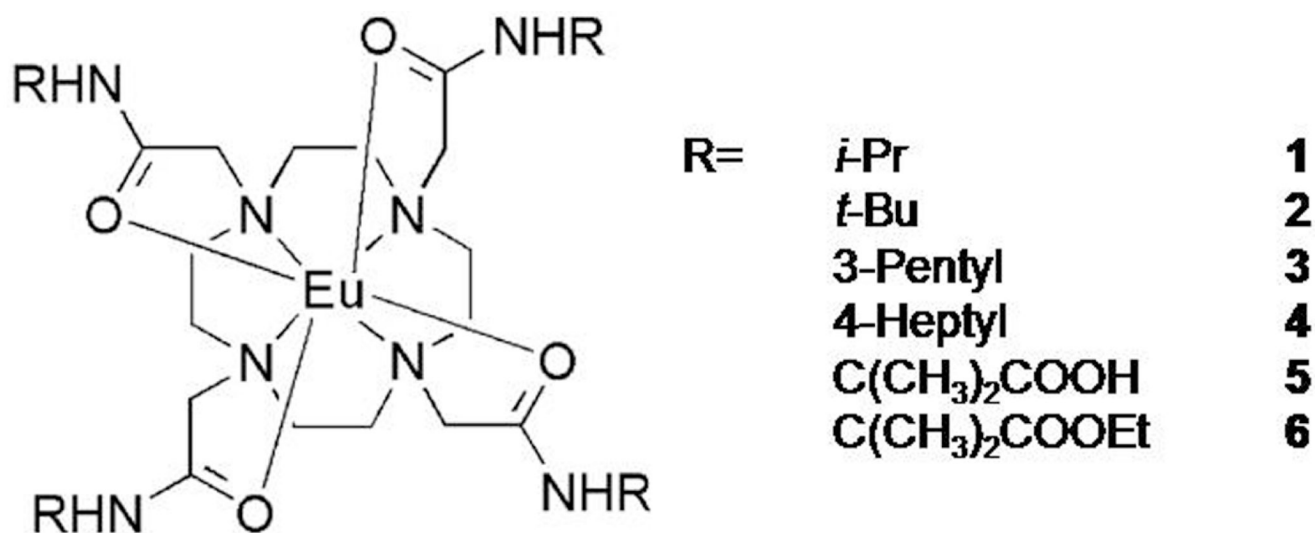


Figure 1.
The Eu(III) DOTA-tetraamide complexes examined in this work.

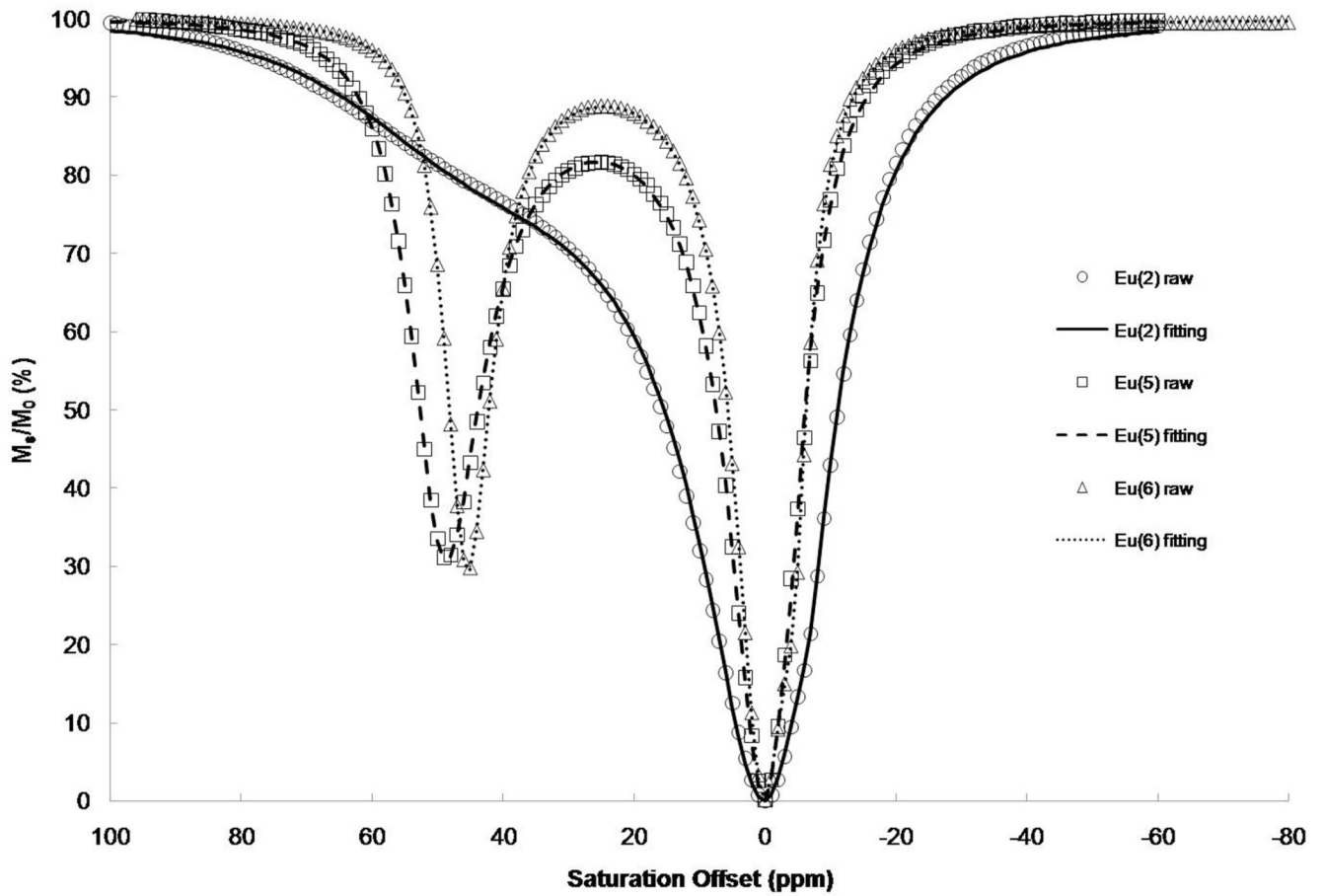


Figure 2. Z-spectra of 40 mM Eu complexes at 500 MHz. The presaturation pulse was a hard square pulse with irradiation time 4s and $B_1 = 23.5 \mu\text{T}$.

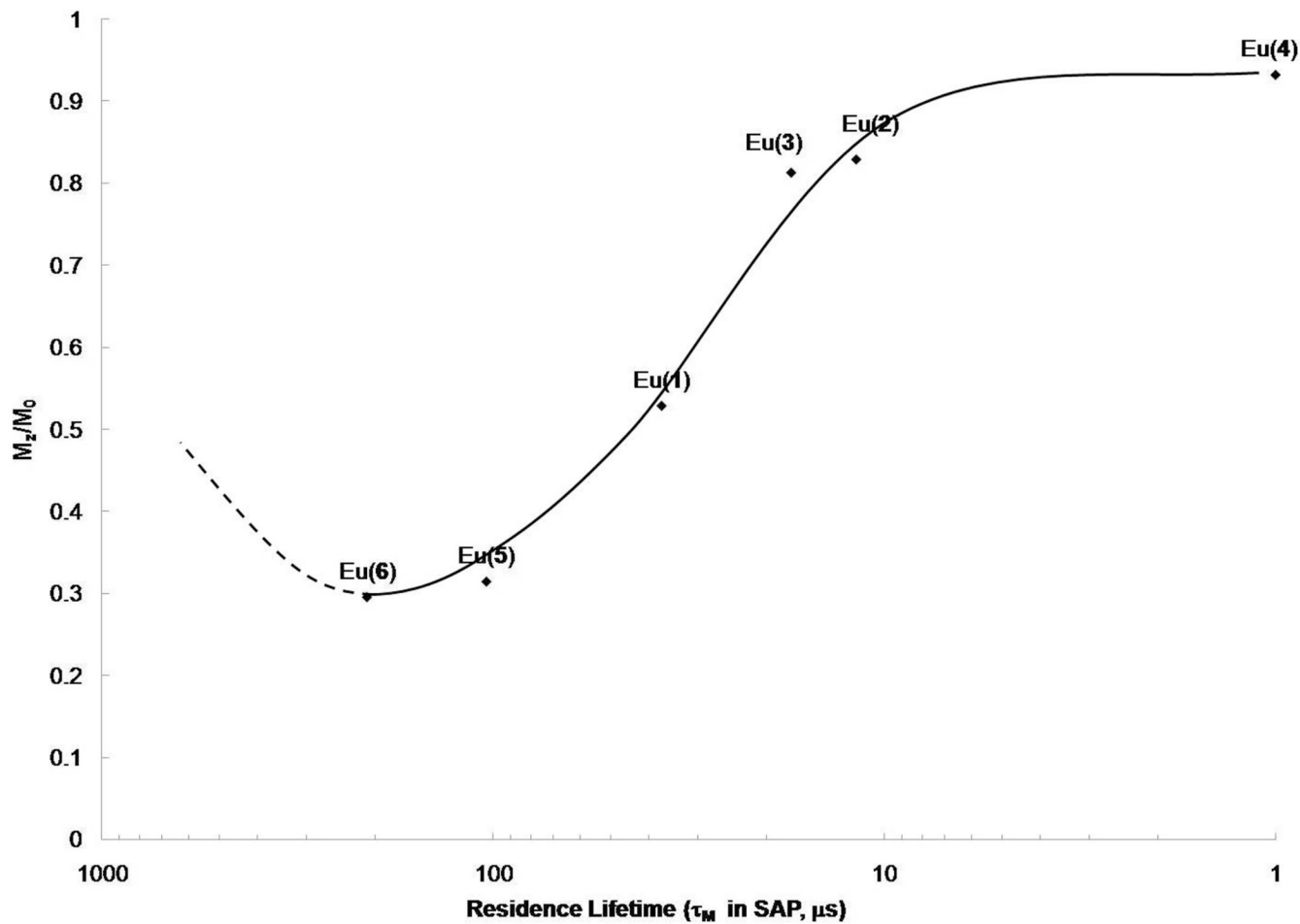


Figure 3.

A plot of the magnitude of the CEST effect (M_z/M_0) measured at 50 ppm (40 mM, 25°C, irradiation time 4s, and $B_1 = 23.5 \mu\text{T}$) versus the experimental Eu(III)-bound water lifetime in each complex. A solid curve was drawn through the data to illustrate the trend while the dashed curve represents the anticipated continuation of this curve based upon theory (8,37).

Isomer ratios, chemical shifts (for SAP isomers) and bound water lifetimes derived from the CEST spectra (irradiation time 4s) for the series of complexes (40 mM) at 25°C.

Table 1

	R =	Charge	SAP/TSAP	τ_M (μs)	$\Delta\omega$ (ppm)	$I-(M_s/M_0)$
1	-CCH(CH ₃) ₂ (<i>i</i> -Pr)	+3	61/39	37	54	0.47
2	-C(CH ₃) ₃ (<i>t</i> -Bu)	+3	61/39	10	50	0.17
3	-CCH(CH ₃)(CH ₂ CH ₃) (β -penyl)	+3	36/64	17	52	0.19
4	-CCH(CH ₂ CH ₂ CH ₂ CH ₃) ₂ (4-heptyl)	+3	23/77	<1	45	0.07
5	-C(CH ₃) ₂ COOH	-1	100/0	104	48	0.69
6	-C(CH ₃) ₂ COOEt	+3	70/30	210	45	0.70

Table 2

Comparisons of the CEST effect as measured by imaging (% decrease in bulk water intensity) between the water and plasma samples of Eu(2), Eu(5) and Eu(6) at different agent concentrations, 20°C, irradiation time 5s and $B_1 = 14.1 \mu\text{T}$.

	1mM	2.5mM	5mM	10mM	20mM
Eu(2) in water	1.2	3.0	5.6	10	18
Eu(2) in plasma	0.8	2.0	3.9	6.4	11
Eu(5) in water	8.7	21	34	49	65
Eu(5) in plasma	8.9	20	33	50	65
Eu(6) in water	5.5	13	23	38	58
Eu(6) in plasma	4.6	13	22	35	55

Table 3

Comparisons of the CEST intensities from spectral data for 10 mM Eu(III) in either water or plasma at four different temperatures. (irradiation time 5s, $B_1 = 18.8 \mu\text{T}$).

Temperature (°C)	27	35	37	39
Water	42	39	37	34
Plasma	41	30	28	25